

Boosting Resolution Generalization of Diffusion Transformers with Randomized Positional Encodings

Cong Liu^{1,2,†,‡}, Liang Hou^{1,†,*}, Mingwu Zheng¹, Xin Tao¹, Pengfei Wan¹, Di Zhang¹, Kun Gai¹

¹Kuaishou Technology ²Southeast University

{liucong08, zhengmingwu, wanpengfei, zhangdi08}@kuaishou.com

{lianghou96, jiangsutx}@gmail.com gai.kun@qq.com



Figure 1. We propose the first **two-dimensional randomized positional encodings** (RPE-2D) specifically designed for diffusion transformers, which significantly improve the resolution generalization without requiring additional training. As shown in the figure, the 512×512 resolution images are generated by the model trained on 256×256 , and the 1024×1024 resolution images are generated by the model trained on 512×512 .

Abstract

Resolution generalization in image generation tasks enables the production of higher-resolution images with lower training resolution overhead. However, a significant challenge in resolution generalization, particularly in the widely used Diffusion Transformers, lies in the mismatch between the positional encodings encountered during testing and those used during training. While existing methods have employed techniques such as interpolation, extrapolation, or their combinations, none have fully resolved this issue. In this paper, we propose a novel two-dimensional randomized positional encodings (RPE-2D) framework that focuses on learning positional order of image patches instead of the specific distances between them, enabling seamless high- and low-resolution image generation without requiring high-

and low-resolution image training. Specifically, RPE-2D independently selects positions over a broader range along both the horizontal and vertical axes, ensuring that all position encodings are trained during the inference phase, thus improving resolution generalization. Additionally, we propose a random data augmentation technique to enhance the modeling of position order. To address the issue of image cropping caused by the augmentation, we introduce corresponding micro-conditioning to enable the model to perceive the specific cropping patterns. On the ImageNet dataset, our proposed RPE-2D achieves state-of-the-art resolution generalization performance, outperforming existing competitive methods when trained at a resolution of 256×256 and inferred at 384×384 and 512×512 , as well as when scaling from 512×512 to 768×768 and 1024×1024 . And it also exhibits outstanding capabilities in low-resolution image generation, multi-stage training acceleration and multi-resolution inheritance.

[†]Equal contribution ^{*}Corresponding author

[‡]Work was done during internship at Kuaishou Technology.

1. Introduction

Diffusion models [13, 21, 28, 29] have effectively replaced traditional models like VAEs [16] and GANs [9] as the dominant technology in the field of image generation due to their outstanding performance [6, 25]. Diffusion Transformers (DiTs) [22] demonstrates that Transformers [33] can effectively scale up within diffusion models, making them a popular research focus in modern diffusion model architectures [2, 5, 18, 19]. However, current image generation models are typically trained at a specific resolution to produce high-quality images at that resolution. As a result, generating high-resolution images requires substantial training costs. This presents a significant challenge when training resources are limited. Consequently, there is a growing need for models that possess the ability to generalize across different resolutions, allowing them to generate high-resolution images without incurring the high training costs typically associated with such tasks.

Currently, various approaches have been proposed to address resolution generalization. The first category of methods [7, 11, 18, 32, 35] aims to enhance network architectures, yet typically yields complex models designed for specific frameworks. The second category of methods [15], improves extrapolation ability by adjusting the attention mechanism to account for variations in attention entropy. However, it overlooks that the one-to-one correspondence introduced by positional encoding, which enables Transformers to perceive token positional information, is a key factor limiting the generalization capacity of DiTs. The third category of methods [1, 18, 23, 36], recognizes the limitations that positional encoding (PE) imposes on extrapolation capabilities, proposing methods such as interpolation, extrapolation, or a combination of both, but they cannot surpass the intrinsic extrapolation limits of the positional encoding itself, and none have fully resolved the gap in positional encodings between training and testing. In this paper, we reframe resolution generalization based on positional encoding and identify that the most critical, yet previously overlooked, aspect in visual tasks is **the order of the positions**, prompting a rethinking of the spatial relationships in visual signals. We identify two key challenges to address. The first is addressing the gap between training and prediction when the model encounters positional encodings it has not seen during the sampling of images for resolution generalization. Second, while the importance of positional encoding order for length extrapolation has been acknowledged and applied in large language models (LLMs) [26], implementing this order effectively in visual tasks for resolution generalization remains both challenging and unexplored.

We argue that to completely resolve the issue of resolution extrapolation, all positional encodings used during testing must be effectively trained. While modifications to positional encodings or attention mechanisms are training-

free, they are ultimately limited by the extrapolation capacity inherent in PE itself. To transcend this limitation, we move beyond traditional PE by proposing a two-dimensional training-based random positional encoding (RPE-2D) inspired by the successful extrapolation applications of one-dimensional random positional encoding (RPE-1D) [26] in LLMs, which reframes the extrapolation problem as a generalized interpolation problem. Our method addresses the positional encoding gap between training and inference, unifying interpolation and extrapolation into a single framework rather than treating them as separate issues. Moreover, it does not require training on high-resolution images, thus avoiding additional training costs. Note that the sampling in RPE-2D fundamentally differs from RPE-1D, as it treats the collected training images as resized or cropped versions of a larger image, where varying intervals and starting points correspond to resizing scale factors and cropping coordinates.

The significance of relative positional information in Transformers highlights the critical role of positional encoding order in visual generation tasks within the DiT architecture, an aspect often overlooked by previous approaches but prioritized in ours. Conventional positional encodings enables the model to perceive positional relationships through the total number of tokens and the distance between adjacent tokens. While the network memorizes intervals and lengths, this is precisely what constrains resolution transcendence. Therefore, we allow lengths and intervals to vary, focusing exclusively on the order of positional encodings. With RPE-2D, we focus on learning positional order rather than distance. However, for images with a two-dimensional structure, it's essential to account for the Euclidean distance in spatial positioning. However, the emphasis on equidistance focuses on position indices, which conflicts with the positional order that RPE-2D aims to learn, posing a challenge in the implementation of order within the context of images.

We utilize RPE-2D to learn the order of positions rather than distances. For images, which have a two-dimensional structure, it is necessary to consider the Euclidean distances that objectively exist in space. Intuitively, there is a need to constrain the equidistance of adjacent token positions. However, equidistance emphasizes position indices, which contradicts the position order that RPE-2D aims to learn, thus creating a challenge in implementing order specifically in images. We have specifically explored how to maintain the topological structure of images while giving the greatest consideration to order, proposing a low-rank order approach. Additionally, we have designed conditioning and enhancement strategies to preserve order. We have specifically explored how to maximize the consideration of order while preserving the topological structure of images. Additionally, we have developed conditioning and enhancement strategies to preserve the order.

In this paper, we propose a novel two-dimensional ran-

dom positional encoding framework that supports both high- and low-resolution generation seamlessly, without requiring high-resolution image training. Beyond resolving the resolution generalization challenge, our reformulation of positional encoding illuminates new avenues for multimodal comprehension and cross-resolution tasks.

2. Related Work

2.1. Length Generalization in LLMs.

A significant stride in extrapolation has been achieved with ALIBI [24], a method that employs local attention to reinforce the model’s ability to capture local dependencies within the data. This is crucial as it allows the model to maintain a more refined understanding of the data’s structure, thereby improving the quality of extrapolation. Another notable approach is the NTK [1], which adjusts the frequency components of the position encodings. This method is designed to preserve the high-frequency information during the extrapolation process, ensuring a more accurate representation of the data’s characteristics. YaRN [23] is an innovative approach that extends the context window of large language models efficiently. It does so by modifying the attention mechanism to handle longer sequences without the need for fine-tuning, thus maintaining a consistent level of performance across various lengths of input data. The concept of random position encoding [26] has also gained traction, offering a more natural and elegant solution to the challenge of handling longer sequences during prediction. This method has been shown to be effective not only in language models but also in non-language models, where the generation of images or other data types requires a broader context understanding. Attention Masking is another strategy that has proven effective in language models, which are inherently local in nature. By “forcing” the model to focus on a limited number of tokens, it can effectively manage the increased complexity during prediction. However, its applicability to non-language models is still under exploration.

2.2. Resolution Generalization in Diffusion Models.

In the realm of computer vision, extrapolation techniques have been pivotal in advancing the capabilities of models to generate images and predict video sequences beyond the limits of their training data. The development of FiT [18] and LuminaNext [36] has showcased the potential of local attention mechanisms in enhancing the performance of image generation models. Local attention focuses on specific regions within an image, allowing for more detailed and accurate generation of high-resolution images. In addition to these, there are modifications to the network structure, such as attention scale [15], neighborhood attention [10], and KV-compression [3].

In summary, while current methods have made limited

improvements in extrapolation capabilities, they still fail to address the fundamental issue of the position encoding gap between training and prediction.

3. Preliminary

3.1. Positional Encodings

Sinusoidal PE Positional encoding (PE) [33] plays a significant role in Transformer-based sequential modeling tasks, as it can assign position information to each token to compensate for the order-unawareness of Transformers. Technically, the widely used sinusoidal PE added the token embedding $\mathbf{x}_m \in \mathbb{R}^d$ at position $m \in \{1, 2, \dots, L\}$ with a positional embedding $\text{PE}(m) := \mathbf{p}_m \in \mathbb{R}^d$ ($d \in \mathbb{N}^+$ is the dimension of embedding), which is formulated as,

$$\text{PE}(m, 2i) := p_{m,2i} = \sin m\theta_i, \quad (1)$$

$$\text{PE}(m, 2i + 1) := p_{m,2i+1} = \cos m\theta_i, \quad (2)$$

where $\theta_i = b^{-2i/d}$ is the frequency on index $i \in \{1, 2, \dots, d/2\}$ with the base $b \in \mathbb{R}^+$.

RoPE Rotary positional encoding (RoPE) [30] is a form of relative position encoding, which demonstrates better length generalization and has become the preferred choice for LLMs and modern DiTs. Specifically, its implementation involves the following transformation applied to the query $\mathbf{q}_m \in \mathbb{R}^d$ at position m and key $\mathbf{k}_n \in \mathbb{R}^d$ at position n in the Self-Attention mechanism (denoted as f),

$$\begin{aligned} f(\mathbf{q}_m, \mathbf{k}_n, m, n) &= (\mathbf{R}_m \mathbf{q}_m)^\top (\mathbf{R}_n \mathbf{k}_n) \\ &= \mathbf{q}_m^\top \mathbf{R}_n^\top \mathbf{R}_m \mathbf{k}_n = \mathbf{q}_m^\top \mathbf{R}_{n-m} \mathbf{k}_n, \end{aligned} \quad (3)$$

where the rotation matrix $\text{RoPE}(n - m) := \mathbf{R}_{n-m} := \mathbf{R}_n^\top \mathbf{R}_m$ is (take 2D-case as example),

$$\mathbf{R}_{n-m} = \begin{pmatrix} \cos(n - m)\theta_i & -\sin(n - m)\theta_i \\ \sin(n - m)\theta_i & \cos(n - m)\theta_i \end{pmatrix}. \quad (4)$$

3.2. 2D Positional Encodings

In general, two-dimensional positional encodings are composed of two independent one-dimensional positional encodings, making them suitable for two-dimensional structures such as images. Taking RoPE-2D as an example, for the query \mathbf{q}_{x_1, y_1} at position (x_1, y_1) and the key \mathbf{k}_{x_2, y_2} at position (x_2, y_2) , the rotation matrix $\text{RoPE}(x_2 - x_1, y_2 - y_1) := \mathbf{R}_{x_2 - x_1, y_2 - y_1}$ is,

$$\mathbf{R}_{x_2 - x_1, y_2 - y_1} = \begin{pmatrix} \mathbf{R}_{x_2 - x_1} & \mathbf{0} \\ \mathbf{0} & \mathbf{R}_{y_2 - y_1} \end{pmatrix}. \quad (5)$$

4. Method

4.1. 2D Randomized Positional Encodings

We study the problem of resolution generalization in image generation, which mainly concerns the case where one

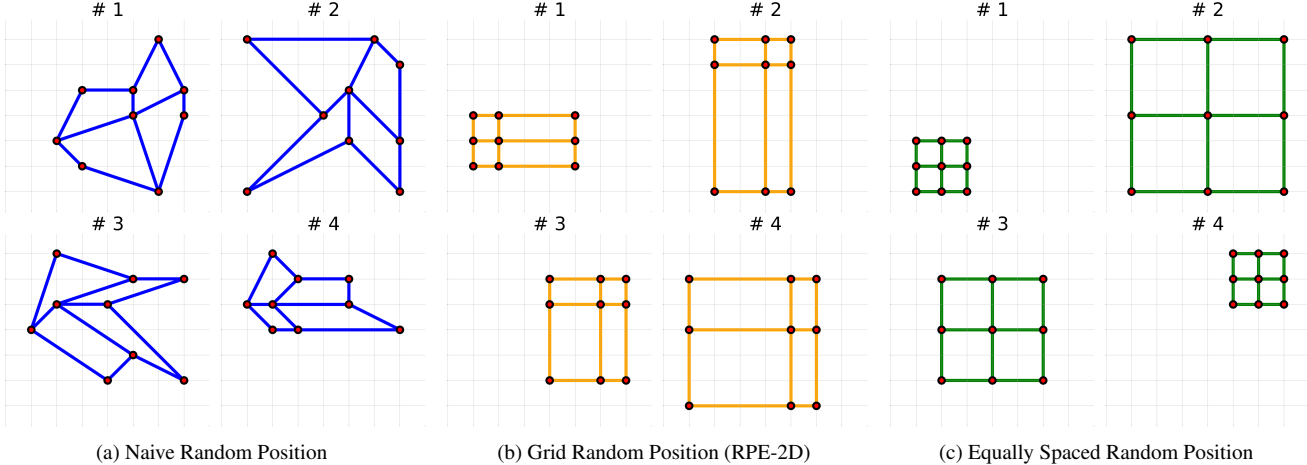


Figure 2. Illustration of different random positions in 2D space. Our RPE-2D is shown in the middle. Our proposed RPE-2D is displayed in the center (Fig(b)), illustrating the balance between randomness and regularity. Fig(c) represents an equidistant RPE-2D counterpart.

can only train at a low resolution due to computational constraints, but wants to sample images at a high resolution. Let $h_{\text{train}} \times w_{\text{train}} \in \mathbb{N}^+ \times \mathbb{N}^+$ be the size of the training images (the VAE encoded latents), and $h_{\text{test}} \times w_{\text{test}} \in \mathbb{N}^+ \times \mathbb{N}^+$ the size of the test images, where $h_{\text{test}} > h_{\text{train}}$ and $w_{\text{test}} > w_{\text{train}}$. It is evident that during resolution extrapolation, this could inevitably result in out-of-distribution positional encodings that extend beyond the training range. NTK [1] and YaRN [23] enhance the model’s capacity for long extrapolation by combining interpolation with extrapolation; however, they still fail to address a core issue: the inconsistency of positional encodings for each token between the training and testing phases. Drawing inspiration from the one-dimensional randomized positional encodings [26] used in LLMs, we reconceptualize the resolution extrapolation problem in image generation as an interpolation task. This idea ensures that the positional encodings during the testing phase remain entirely within the training distribution. By sequentially and randomly selecting the positional encodings for image patches, we ensure that all positional encodings during the testing phase have been previously trained, thereby enhancing the model’s robustness on positions of patches.

To the best of our knowledge, we are the first to apply randomized positional encodings to DiT-based image generation. This requires us to extend the one-dimensional randomized positional encodings originally designed for text modalities into two-dimensional random positional encodings suitable for image modalities. The most straightforward approach would be to flatten the image patches into a one-dimensional sequence and then randomly sample positions corresponding to the number of image patches within a larger sequence length of HW , where $H > h_{\text{test}} > h_{\text{train}}$ and $W > w_{\text{test}} > w_{\text{train}}$ are preset hyper-parameters. How-

ever, this completely disregards the prior knowledge of the two-dimensional spatial structure of the image, resulting in distorted distance measurements between positions in the vertical and horizontal directions (see Figure 2(a)).

For two-dimensional image data, the horizontal and vertical axes are decoupled. Therefore, in this paper, we propose to perform independent random position sampling along the horizontal and vertical axes of the image. Specifically, for each training step, we sample without replacement a random set of indices $\mathcal{X} \subset \{1, 2, \dots, H\}$, $\mathcal{Y} \subset \{1, 2, \dots, W\}$ along the horizontal and vertical axes of the image such that $|\mathcal{X}| = h_{\text{train}}$ and $|\mathcal{Y}| = w_{\text{train}}$. We then sort \mathcal{X} and \mathcal{Y} in ascending order, such that $\mathcal{X} = \{x_1, \dots, x_{h_{\text{train}}}\}$ for $x_1 < x_2 < \dots < x_{h_{\text{train}}}$ and $\mathcal{Y} = \{y_1, \dots, y_{w_{\text{train}}}\}$ for $y_1 < y_2 < \dots < y_{w_{\text{train}}}$. And then constructing 2D random positions through the Cartesian product, which is defined as follows,

$$\mathcal{X} \times \mathcal{Y} = \{(x, y) \mid x \in \mathcal{X}, y \in \mathcal{Y}\}. \quad (6)$$

Correspondingly, the randomized positional encoding for patch at position $1 \leq i \leq h_{\text{train}}$, $1 \leq j \leq w_{\text{train}}$ during training is computed as $\text{RPE}(i, j) := \text{PE}(x_i, y_j) \in \mathbb{R}^d$, where $(x_i, y_j) \subseteq \mathcal{X} \times \mathcal{Y}$ (take PE as example). This method not only ensures the order between the horizontal and vertical axes, but also ensures the consistency within each horizontal and vertical axis of the image, i.e., the vertical coordinates in each horizontal axis are consistent, and the horizontal coordinates in each vertical axis are consistent. (see Figure 2(b)). At test time, the position selection is deterministic and maximally equidistant, i.e., $x_1 = 1$, $x_{h_{\text{test}}} = H$, $y_1 = 1$, $y_{w_{\text{test}}} = W$, $x_{i+1} - x_i = \lfloor H/h_{\text{test}} \rfloor$, and $y_{i+1} - y_i = \lfloor W/w_{\text{test}} \rfloor$. It is also noteworthy that our 2D random positional encoding training paradigm is applicable to various existing positional encoding methods, including Sinusoidal PE and RoPE. We

validated this property in our experiments.

Inspired by the inference setup, we further explore the concept of equidistant randomized positional encoding (see Figure 2(c)). Specifically, during each instance of random positional sampling in the training process, the intervals within both the horizontal and vertical axes are kept consistent, with only the interval size and starting position being randomly determined. Mathematically, we have $r = x_{i+1} - x_i = x_i - x_{i-1} = y_{i+1} - y_i = y_i - y_{i-1}$, where r , x_1 , and y_1 are randomly determined within the specified range. This approach represents a further regularization of RPE-2D. However, due to its stronger regularity, it introduces the risk of reducing the model’s ability to perceive the positional order between image patches. We provide a comparison of this method versus RPE-2D in Appendix.

4.2. Data Augmentation and Micro-Conditioning

To further enhance the model’s ability to perceive the order of image patches, we simultaneously use resize and crop operations to adjust the “collected” high-resolution images into low-resolution images suitable for actual training. The resize operation helps the model capture the global structure, while the crop operation encourages the model to focus on local details. Notably, the low-resolution images produced by these two operations have equal areas. Additionally, we have designed a micro-conditional injection logic to address the issue of image incompleteness caused by cropping. Initially, we upscale the low-resolution images in the training dataset to a high resolution (if necessary) and record the base size as $\mathbf{c}_{\text{original}} = (h_{\text{original}}, w_{\text{original}})$. During each training session, we randomly select starting and ending coordinate points from the available cropping options (including no cropping for global resizing) and crop the base image accordingly, obtaining the crop coordinates $\mathbf{c}_{\text{crop}} = (c_{\text{top}}, c_{\text{left}}, c_{\text{down}}, c_{\text{right}})$. After cropping, we resize the extracted region so that the resulting $\mathbf{c}_{\text{resize}} = (h_{\text{target}}, w_{\text{target}})$ such that the product $h_{\text{target}} \times w_{\text{target}}$ meets the required training resolution. These three types of conditional information are injected into the model via adaLN [34]. Each component is independently embedded using a Fourier feature encoding [31], and these embeddings are concatenated into a single vector that we feed into the model by adding it to the timestep embedding of DiT [22].

4.3. Training-free Sampling Strategy

Attention Scale In addition to the changes in position encoding, resolution extrapolation inevitably leads to an increase in the number of patches, creating another inconsistency between testing and training. Since attention is scale-dependent, this dependency arises from the fact that the entropy of attention changes as the number of patches increases [15]. We also attempt to use the proposed scaling

factor to mitigate the variations in attention entropy.

$$\text{Attention}(\mathbf{Q}, \mathbf{K}, \mathbf{V}) = \text{softmax} \left(\frac{\log_n m}{\sqrt{d}} \mathbf{Q} \mathbf{K}^\top \right) \mathbf{V}, \quad (7)$$

where $m = h_{\text{test}} \times w_{\text{test}}$ and $n = h_{\text{train}} \times w_{\text{train}}$ represent the number of patches during testing and training respectively.

Timestep Shift When generating large images with diffusion models, the increase in resolution leads to an increase in the noise schedule signal-to-noise ratio (SNR) used in training [14]. Therefore, it is necessary to adjust the inference timestep spacing during sampling to maintain the SNR as much as possible. Specifically, We follow SD3 [8] to map the time step $t_n \in \{1, 2, \dots, T\}$ for n patches in training to the time step $t_m \in \{1, 2, \dots, T\}$ for m patches in inference in order to approximate the same level of SNR.

$$t_m = \left\lfloor \frac{\sqrt{\frac{m}{n}} \times \frac{t_n}{T}}{1 + \left(\sqrt{\frac{m}{n}} - 1 \right) \times \frac{t_n}{T}} \right\rfloor \times T. \quad (8)$$

5. Experiments

5.1. Experimental Setup

Training We follow the DiT [22] by using ImageNet 256×256 and ImageNet 512×512 as training datasets, employing the DiT-XL/2 network architecture while keeping the other training hyper-parameters unchanged. On the ImageNet 256×256 , we train from scratch the models for 400k iterations with our proposed randomized positional encoding to compare with baselines. Subsequently, we fine-tune on ImageNet 512×512 based on the weights at the 400k training step from ImageNet 256×256 , conducting an additional 800k iterations, and compare the results of resolution extrapolation with baseline methods.

Evaluation Following DiT, we use FID [12], sFID [20], IS [27], and Precision/Recall [17] as the quantitative evaluation metrics in the experiments. The “cfg-scale” in our experiments is set to the default value of 4.0 in `sample.py` from DiT’s official code initially.

5.2. Comparisons

RPE-2D is a training approach for positional encodings rather than a specific positional encoding form, making it theoretically compatible with any types of positional encoding. We initially implemented comparison of RPE-2D applied on SinPE and RoPE, as shown in Table 3, which demonstrates that both position encodings combined with RPE-2D resulted in gains.

<https://github.com/facebookresearch/DiT>

Table 1. Comparison of RPE-2D with different methods on resolution extrapolation trained ImageNet 256×256

Method	ImageNet 256×256									
	384×384					512×512				
	FID↓	sFID↓	IS↑	Prec.↑	Rec.↑	FID↓	sFID↓	IS↑	Prec.↑	Rec.↑
PI	18.87	41.59	260.97	0.8312	0.0602	30.64	57.76	159.72	0.676	0.055
Ext	15.95	37.79	374.74	0.8970	0.0636	28.35	54.77	232.41	0.607	0.181
NTK	16.56	35.92	375.28	0.9203	0.0686	27.88	49.8	227.45	0.619	0.177
YaRN	16.97	26.08	264.34	0.7864	0.1050	19.13	34.31	253.16	0.749	0.151
RPE-2D	15.63	14.40	385.67	0.9631	0.1174	17.95	18.23	348.99	0.849	0.181

Table 2. Comparison of RPE-2D with different methods on resolution extrapolation trained ImageNet 512×512

Method	ImageNet 512×512									
	768×768					1024×1024				
	FID↓	sFID↓	IS↑	Prec.↑	Rec.↑	FID↓	sFID↓	IS↑	Prec.↑	Rec.↑
PI	27.24	68.63	150.53	0.8441	0.373	38.64	92.49	139.38	0.7066	0.361
Ext	20.57	53.65	223.39	0.8184	0.462	45.77	116.54	180.16	0.5698	0.499
NTK	21.58	46.11	225.00	0.7883	0.452	32.90	73.69	216.12	0.6304	0.579
YaRN	55.21	75.84	62.93	0.5547	0.513	50.65	79.04	103.38	0.6010	0.461
RPE-2D	20.45	40.46	271.05	0.8271	0.512	25.40	47.18	192.05	0.8109	0.535

We then compared RPE-2D with NTK [1], YaRN [23], PI [4], and Ext, in conjunction with RoPE [30] on resolution extrapolation. It is worth noting that our comparisons are all based on two-dimensional positional encodings, *e.g.*, NTK and YaRN are modified by Equation 5 following FiT [18] as “2D version”. We extrapolated to 384×384 and 512×512 resolutions using the weights at the 400k iterations from ImageNet 256×256 . As shown in Table 1, RPE-2D achieved state-of-the-art metrics in both 384×384 and 512×512 resolutions, decreasing the previous best sFID of **34.31** achieved by YaRN to **18.23**, exhibiting advanced achievement in resolution extrapolation. As shown in Figure 3, RPE-2D still maintains a superior quality when extrapolating to a resolution of 512×512 , which demonstrates that we have effectively increased the upper limit of extrapolation compared to YaRN and NTK.

Subsequently, we employ the weights fine-tuned on ImageNet 512×512 for an additional 800k iterations to extrapolate to 768×768 and 1024×1024 resolutions. Table 2 shows that RPE-2D sustains its preeminent position in extrapolation to higher resolutions, while PI [4] achieves good performance in Prec. Figure 3 presents a qualitative comparison between our method and baseline approaches. Only our method consistently preserves both structure and detail across various resolutions. In contrast, methods like NTK and YaRN, which combine interpolation and extrapolation, particularly exhibit structural errors. While PI, as an interpolation method, suffers from a loss of detail.

5.3. Ablation Studies

We conduct an ablation study over the main components of RPE-2D: (i) random augmentation and micro-conditioning (Cond-Aug) (ii) attention scale (iii) timestep shift.

Our newly proposed Cond-Aug treats the collected low-resolution training images as resized or cropped versions of larger images, where varying intervals and starting points correspond to resizing scale factors and cropping coordinates. As demonstrated in Table 4, Cond-Aug reduces the FID from **20.78** to **19.12** and improves the IS from **293.96** to **325.76**, leading to substantial performance improvement at extrapolated resolutions, indicating its enhancement for position’s ordering modeling. Additionally, our strategically incorporated attention scale and timestep shift yield a substantial improvement in IS alongside a significant reduction in sFID, as reported in Table 4, demonstrating their enhancement for RPE-2D.

In Appendix, we also train RPE-2D for a wide range of different maximum positions $H = W \subset \{64, 128, 256, 512, 1024\}$. The experiments suggest that RPE-2D’s performance is largely unaffected by the precise value of the maximum position.

5.4. Applications

In this subsection, we show that RPE-2D can generate images at low-resolution, and accelerate convergence when continuing to train at high resolutions. Multi-ratio generation results are shown in Appendix.



Figure 3. Qualitative results of RPE-2D against different position encoding extrapolation baselines at different resolutions.

Table 3. Comparison of RPE-2D applied on different position encoding forms (SinPE and RoPE).

Method	ImageNet 256×256					ImageNet 512×512				
	FID↓	sFID↓	IS↑	Prec.↑	Rec.↑	FID↓	sFID↓	IS↑	Prec.↑	Rec.↑
SinPE	17.82	11.33	359.32	0.927	0.149	14.75	10.02	277.92	0.8341	0.143
RoPE	17.30	11.07	366.19	0.956	0.176	14.17	7.16	313.73	0.8677	0.176
SinPE + RPE-2D	17.33	11.21	358.43	0.931	0.155	14.53	8.72	302.55	0.8324	0.145
RoPE + RPE-2D	16.92	11.02	362.14	0.959	0.170	14.09	6.61	398.35	0.8399	0.225

5.4.1. Low-Resolution Image Generation

As shown in Figure 4, RPE-2D can not only generate images with higher resolution than the training images, but also generate images with lower resolution images, such as generating 128×128 images when the training resolution is 256×256 . This demonstrates the resolution generalization ability of RPE-2D both upwards and downwards.

5.4.2. Multi-Stage Training Acceleration

Due to the ability of RPE-2D to achieve high-quality high-resolution images from training at low resolutions, an intuitive application is to facilitate multi-resolution convergence. We fine-tuned a model of size 256 using ImageNet at a resolution of 512×512 and compared the impact of RoPE and RPE-2D with our random positional encoding scheme on the

Table 4. Ablation study over the main components of RPE-2D. Ablation components are progressively integrated in sequence. For example, “+Timestep Shift” indicates the full configuration incorporating Cond-Aug, Attention Scale, and Timestep Shift into the base RPE-2D.

Method	ImageNet 256×256									
	256×256					512×512				
	FID↓	sFID↓	IS↑	Prec.↑	Rec.↑	FID↓	sFID↓	IS↑	Prec.↑	Rec.↑
RPE-2D	17.17	11.19	358.17	0.9579	0.1683	20.78	27.29	293.96	0.8155	0.155
+ Cond-Aug	17.09	11.13	359.55	0.9587	0.1687	19.12	23.91	325.76	0.8399	0.163
+ Attention Scale	17.02	11.05	361.73	0.9578	0.1693	18.33	19.17	347.82	0.8469	0.177
+ Timestep Shift	16.92	11.02	362.14	0.9591	0.1703	17.95	18.23	348.99	0.8493	0.181



Figure 4. Generates images at different resolutions, including 128×128 , 256×256 , 512×512 , 768×768 , and 1024×1024 .

loss convergence process. The results shown in Figure 5 that our random positional encoding scheme starts with a lower loss and exhibits better convergence, which is beneficial for staged training of large models.

6. Conclusion

This work mainly investigates the resolution extrapolation problem in diffusion transformers (DiTs) from the perspective of positional encoding. Previously related approaches

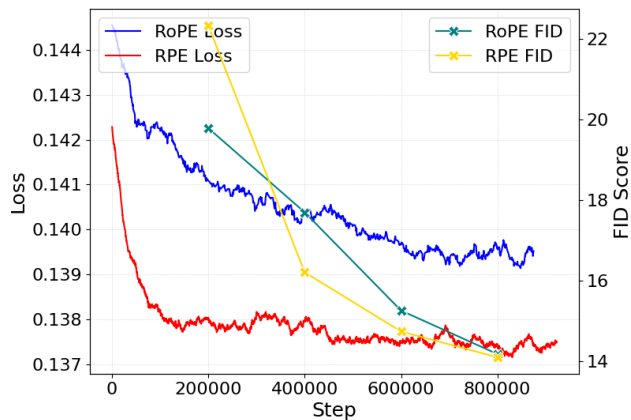


Figure 5. Training loss and FID curves of RoPE and RPE-2D.

such as NTK and YaRN have not fully addressed the inconsistency of positional encodings between training and testing phases. We propose an 2D randomized positional encoding for DiTs, ensuring that the positional encodings during testing are all trained. By modeling the position orders among image patches rather than their absolute distances, our method bridge the gap between training and testing. Additionally, we propose random data augmentation further enhance the model’s ordering modeling while reducing its dependency on the exact number of tokens. To address the potential issue of image incompleteness caused by random data augmentation, we also introduce micro-conditioning, enabling the model to perceive the specific augmentation methods applied. During high-resolution inference, we also employ attention scaling and timestep shifting to address issues related to attention entropy increase and signal-to-noise ratio mismatch. Experimental results on ImageNet-256/512 demonstrate that our proposed method significantly outperforms existing competing approaches in the resolution generalization problem. In the future, we will extend the proposed method to text-to-image and text-to-video tasks.

References

- [1] Ntk-aware scaled rope allows llama models to have extended (8k+) context size without any fine-tuning and minimal perplexity degradation. http://www.reddit.com/r/LocalLLaMA/comments/141z7j5/ntkaware_scaled_rope_, 2024. Accessed: 2024-4-10. 2, 3, 4, 6
- [2] Junsong Chen, Jincheng Yu, Chongjian Ge, Lewei Yao, Enze Xie, Yue Wu, Zhongdao Wang, James Kwok, Ping Luo, Huchuan Lu, et al. Pixart-alpha: Fast training of diffusion transformer for photorealistic text-to-image synthesis. *arXiv preprint arXiv:2310.00426*, 2023. 2
- [3] Junsong Chen, Chongjian Ge, Enze Xie, Yue Wu, Lewei Yao, Xiaozhe Ren, Zhongdao Wang, Ping Luo, Huchuan Lu, and Zhenguo Li. Pixart-sigma: Weak-to-strong training of diffusion transformer for 4k text-to-image generation. *arXiv preprint arXiv:2403.04692*, 2024. 3
- [4] Shouyuan Chen, Sherman Wong, Liangjian Chen, and Yuandong Tian. Extending context window of large language models via positional interpolation. *arXiv preprint arXiv:2306.15595*, 2023. 6
- [5] Shoufa Chen, Mengmeng Xu, Jiawei Ren, Yuren Cong, Sen He, Yanping Xie, Animesh Sinha, Ping Luo, Tao Xiang, and Juan-Manuel Perez-Rua. Gentron: Diffusion transformers for image and video generation. In *Proceedings of the IEEE/CVF Conference on Computer Vision and Pattern Recognition*, pages 6441–6451, 2024. 2
- [6] Prafulla Dhariwal and Alexander Nichol. Diffusion models beat gans on image synthesis. *Advances in neural information processing systems*, 34:8780–8794, 2021. 2
- [7] Ruoyi Du, Dongliang Chang, Timothy Hospedales, Yi-Zhe Song, and Zhanyu Ma. Demofusion: Democratizing high-resolution image generation with no \$\$\$\$. In *Proceedings of the IEEE/CVF Conference on Computer Vision and Pattern Recognition*, pages 6159–6168, 2024. 2
- [8] Patrick Esser, Sumith Kulal, Andreas Blattmann, Rahim Entezari, Jonas Müller, Harry Saini, Yam Levi, Dominik Lorenz, Axel Sauer, Frederic Boesel, et al. Scaling rectified flow transformers for high-resolution image synthesis. In *Forty-first International Conference on Machine Learning*, 2024. 5
- [9] Ian Goodfellow, Jean Pouget-Abadie, Mehdi Mirza, Bing Xu, David Warde-Farley, Sherjil Ozair, Aaron Courville, and Yoshua Bengio. Generative adversarial nets. *Advances in neural information processing systems*, 27, 2014. 2
- [10] Ali Hassani, Steven Walton, Jiachen Li, Shen Li, and Humphrey Shi. Neighborhood attention transformer. In *Proceedings of the IEEE/CVF Conference on Computer Vision and Pattern Recognition*, pages 6185–6194, 2023. 3
- [11] Yingqing He, Shaoshu Yang, Haoxin Chen, Xiaodong Cun, Menghan Xia, Yong Zhang, Xintao Wang, Ran He, Qifeng Chen, and Ying Shan. Scalecrafter: Tuning-free higher-resolution visual generation with diffusion models. In *The Twelfth International Conference on Learning Representations*, 2023. 2
- [12] Martin Heusel, Hubert Ramsauer, Thomas Unterthiner, Bernhard Nessler, and Sepp Hochreiter. Gans trained by a two time-scale update rule converge to a local nash equilibrium. *Advances in neural information processing systems*, 30, 2017. 5
- [13] Jonathan Ho, Ajay Jain, and Pieter Abbeel. Denoising diffusion probabilistic models. *Advances in neural information processing systems*, 33:6840–6851, 2020. 2
- [14] Emiel Hoogeboom, Jonathan Heek, and Tim Salimans. simple diffusion: End-to-end diffusion for high resolution images. In *International Conference on Machine Learning*, pages 13213–13232. PMLR, 2023. 5
- [15] Zhiyu Jin, Xuli Shen, Bin Li, and Xiangyang Xue. Training-free diffusion model adaptation for variable-sized text-to-image synthesis. *Advances in Neural Information Processing Systems*, 36:70847–70860, 2023. 2, 3, 5
- [16] Diederik P Kingma. Auto-encoding variational bayes. *arXiv preprint arXiv:1312.6114*, 2013. 2
- [17] Tuomas Kynkäänniemi, Tero Karras, Samuli Laine, Jaakko Lehtinen, and Timo Aila. Improved precision and recall metric for assessing generative models. *Advances in neural information processing systems*, 32, 2019. 5
- [18] Zeyu Lu, Zidong Wang, Di Huang, Chengyue Wu, Xihui Liu, Wanli Ouyang, and Lei Bai. Fit: Flexible vision transformer for diffusion model. *arXiv preprint arXiv:2402.12376*, 2024. 2, 3, 6
- [19] Nanye Ma, Mark Goldstein, Michael S Albergo, Nicholas M Boffi, Eric Vanden-Eijnden, and Saining Xie. Sit: Exploring flow and diffusion-based generative models with scalable interpolant transformers. *arXiv preprint arXiv:2401.08740*, 2024. 2
- [20] Charlie Nash, Jacob Menick, Sander Dieleman, and Peter W Battaglia. Generating images with sparse representations. *arXiv preprint arXiv:2103.03841*, 2021. 5
- [21] Alexander Quinn Nichol and Prafulla Dhariwal. Improved denoising diffusion probabilistic models. In *International conference on machine learning*, pages 8162–8171. PMLR, 2021. 2
- [22] William Peebles and Saining Xie. Scalable diffusion models with transformers. In *Proceedings of the IEEE/CVF International Conference on Computer Vision*, pages 4195–4205, 2023. 2, 5
- [23] Bowen Peng, Jeffrey Quesnelle, Honglu Fan, and Enrico Shippole. Yarn: Efficient context window extension of large language models. *arXiv preprint arXiv:2309.00071*, 2023. 2, 3, 4, 6
- [24] Ofir Press, Noah A Smith, and Mike Lewis. Train short, test long: Attention with linear biases enables input length extrapolation. *arXiv preprint arXiv:2108.12409*, 2021. 3
- [25] Robin Rombach, Andreas Blattmann, Dominik Lorenz, Patrick Esser, and Björn Ommer. High-resolution image synthesis with latent diffusion models. In *Proceedings of the IEEE/CVF conference on computer vision and pattern recognition*, pages 10684–10695, 2022. 2
- [26] Anian Ruoss, Grégoire Delétang, Tim Genewein, Jordi Grau-Moya, Róbert Csordás, Mehdi Bannani, Shane Legg, and Joel Veness. Randomized positional encodings boost length generalization of transformers. *arXiv preprint arXiv:2305.16843*, 2023. 2, 3, 4

- [27] Tim Salimans, Ian Goodfellow, Wojciech Zaremba, Vicki Cheung, Alec Radford, and Xi Chen. Improved techniques for training gans. *Advances in neural information processing systems*, 29, 2016. [5](#)
- [28] Jiaming Song, Chenlin Meng, and Stefano Ermon. Denoising diffusion implicit models. *arXiv preprint arXiv:2010.02502*, 2020. [2](#)
- [29] Yang Song, Jascha Sohl-Dickstein, Diederik P Kingma, Abhishek Kumar, Stefano Ermon, and Ben Poole. Score-based generative modeling through stochastic differential equations. *arXiv preprint arXiv:2011.13456*, 2020. [2](#)
- [30] Jianlin Su, Murtadha Ahmed, Yu Lu, Shengfeng Pan, Wen Bo, and Yunfeng Liu. Roformer: Enhanced transformer with rotary position embedding. *Neurocomputing*, 568:127063, 2024. [3](#), [6](#)
- [31] Matthew Tancik, Pratul Srinivasan, Ben Mildenhall, Sara Fridovich-Keil, Nithin Raghavan, Utkarsh Singhal, Ravi Ramamoorthi, Jonathan Barron, and Ren Ng. Fourier features let networks learn high frequency functions in low dimensional domains. *Advances in neural information processing systems*, 33:7537–7547, 2020. [5](#)
- [32] Piotr Teterwak, Aaron Sarna, Dilip Krishnan, Aaron Maschinot, David Belanger, Ce Liu, and William T Freeman. Boundless: Generative adversarial networks for image extension. In *Proceedings of the IEEE/CVF International Conference on Computer Vision*, pages 10521–10530, 2019. [2](#)
- [33] A Vaswani. Attention is all you need. *Advances in Neural Information Processing Systems*, 2017. [2](#), [3](#)
- [34] Jingjing Xu, Xu Sun, Zhiyuan Zhang, Guangxiang Zhao, and Junyang Lin. Understanding and improving layer normalization. *Advances in neural information processing systems*, 32, 2019. [5](#)
- [35] Zongxin Yang, Jian Dong, Ping Liu, Yi Yang, and Shuicheng Yan. Very long natural scenery image prediction by outpainting. In *Proceedings of the IEEE/CVF international conference on computer vision*, pages 10561–10570, 2019. [2](#)
- [36] Le Zhuo, Ruoyi Du, Han Xiao, Yangguang Li, Dongyang Liu, Rongjie Huang, Wenzhe Liu, Lirui Zhao, Fu-Yun Wang, Zhanyu Ma, et al. Lumina-next: Making lumina-t2x stronger and faster with next-dit. *arXiv preprint arXiv:2406.18583*, 2024. [2](#), [3](#)